JOURNAL OF APPLIED POLYMER SCIENCE VOL. 21, 3381–3405 (1977)

Heterogeneous Network Polymers. IV. Dynamic Mechanical Properties—Composition—Phase Structure Relationships

TETSUO MORI, KATSUMI OGAWA, and TAKEHIDE TANAKA,
Department of Materials Science and Technology, Kyushu University, Fukuoka, Japan 812

Synopsis

Heterogeneous network polymers were prepared from poly(D-glutamic acid) (PGA) and poly(oxyethylene glycol) (PEG). The content of PGA was systematically varied: 30%, 40%, 50%, 60%, 65%, and 70% by weight. The molecular weights of the crosslinking PEG were 300, 600, 900, and 1800. The plots of the dynamic mechanical tan δ peak temperatures, the PGA interhelical distances (x-rays) and the densities against PGA contents showed a distinct break between 50% and 60%. The photographs under polarizing microscope also indicated an occurrence of phase inversion in the above content region. PGA containing small amounts of PEG and PEG containing small amounts of PGA were found to constitute the continuous phases, respectively, above and below the phase inversion region, while a well-mixed phase is always the dispersed phase. The glass transition was ascribed to the micro-Brownian motions of PGA, PEG, and PEG above and below the phase inversion region, respectively.

INTRODUCTION

Many commercially important plastics and rubbers are prepared by the methods of polymer blends, block, or graft copolymerization. These materials are endowed with more desirable properties by combination of the properties of each component polymer. In general, the component polymers are incompatible with each other, one of them being a hard-component polymer and the other, a soft-component polymer. It is well known that the properties of these materials depend on the glass transition temperatures of the component homopolymers, the composition, the domain structure resulting from incompatibility, the synthetic conditions (temperature, concentration, solvent, and the rate of evaporation of the solvent), etc.[1–6]

We have been interested in the preparation and the physical properties of heterogeneous network polymers which are composed of different polymeric chains. We chose synthetic polypeptides and polyethers as hard- and soft-component polymers, respectively. Synthetic polypeptides in the solid state exhibit characteristic properties as they can retain various secondary structure such as α-helix, β-form, and random coil owing to the intra- and intermolecular hydrogen bonds. Polyethers have been widely used as a soft component in polyurethane elastomers.

In the previous papers,[7–9] we showed that poly(ε-N-carbobenzoxy-L-lysine) and poly(L-glutamic acid) can be crosslinked with isocyanate-terminated polyethers and poly(oxyethylene glycol), respectively, and we discussed mainly the relation between the glass transition temperature and the composition. It was found that the dynamic mechanical properties of heterogeneous network polymers were greatly influenced by several factors such as the relative content of a polypeptide and a polyether, the compatibility of the polypeptide with the polyether, the crosslink density, and the concentration of free carboxyl groups. As mentioned above, however, the physical properties of this type of polymers may also be greatly influenced by the domain structure.

In this paper, we describe the dynamic mechanical properties—composition–domain structure relationships based on dynamic mechanical measurements, infrared spectra, wide-angle x-ray diffraction patterns, and polarizing microscopy. In the present work, we chose poly(glutamic acid) (PGA) and poly(oxyethylene glycol) (PEG) as hard- and soft-component polymers, respectively. The heterogeneous network polymers were synthesized by esterification of carboxyl groups in PGA with the hydroxyl groups in PEG in the absence of catalysts. A series of the heterogeneous network polymers have been prepared by systematically varying the PGA content and the molecular weight of PEG.

EXPERIMENTAL

Materials

Poly(D-glutamic acid) (PGA) prepared by saponification of poly(γ-methyl D-glutamate) had a molecular weight in the range of 42,000–46,000. The extent of hydrolysis determined by quantitative analysis of methoxy groups (Zeisel method) was 97%–99%.

Poly(oxyethylene glycol) (PEG) had number-average molecular weights of 330, 570, 880, and 1830, which will be designated as PEG300, PEG600, PEG900, and PEG1800, respectively. Heterogeneous network polymers with systematically varied PGA content as 30%, 40%, 50%, 60%, 65%, 70% by weight were synthesized. For example, 2.00 g PGA was dissolved in 21 ml N,N-dimethylformamide (DMF) at 100°C. Then, 1.32 g PEG was added and dissolved. The clear solution was poured onto a mold coated with fluoride varnishes. The mold was placed in an airtight metal box and heated in an oven for two to three days at 100°C. The box was then opened to allow DMF to evaporate slowly—it usually took three to four more days until DMF was completely gone. For convenience, we hereafter use the designation PGA-PEG300 (60/40) to represent a heterogeneous network polymer made of PGA and PEG300 at 60 and 40 wt %, respectively. At least two films of network polymers having the same composition were synthesized to check the reproducibility of the properties except for PGA-PEG1800 (70/30), for which we could prepare only once.

Apparatus and Procedures

Dynamic mechanical measurements were made with a Model DDV-IIC Rheovibron at 110 Hz in the temperature range of −120°–200°C. The temperature was raised at a rate of 1.5–2°C/min.

TABLE I
Reaction of PGA with TEGME

PGA-TEGME no.	$1/K$[a]	Found,[b] %			Calcd.,[b] %			ρ,[c] %
		C	H	N	C	H	N	
1	1.0	49.79	6.61	8.33	49.79	6.55	8.29	24.9
2	2.0	50.65	6.91	7.33	50.65	6.88	7.51	35.8
3	5.0	51.00	7.06	7.10	51.00	7.00	7.23	40.3

[a] K = [—COOH]/[—OH], mole ratio of carboxyl groups in PGA to hydroxyl groups in original reaction mixtures.
[b] Elemental analysis.
[c] Degree of esterification reaction calculated by carbon content.

Wide-angle x-ray diffraction patterns were obtained with a Rigaku Denki Type D-3F x-ray generator. Nickel-filtered CuK_α radiation was used at 35 kV and 15 mA.

A Nikon polarizing optical microscope Type POH was used to observe the domain structure or optical anisotropy. Micrographs of cross sections of thin specimens approximately 50 microns thick, sectioned with the use of a razor blade, were taken.

Infrared absorption spectra of the network polymers were measured on a Perkin-Elmer Model 567 spectrophotometer using a multiple internal reflection (MIR) accessory.

Swelling measurements were made as follows. Samples of about 0.15 g were allowed to swell in DMF for seven days at 25°C. Then, the swollen samples were weighed and dried to constant weights at 100°C. Swelling ratio q and gel percent g were determined from equations

$$q = 1 + (W_a - W_b)d_p/W_a d_s$$

and

$$g = W_b/W \times 100$$

where W is the weight of the unswollen network polymer, W_a is the weight of the swollen gel, W_b is the weight of the dry gel, d_p is the density of the network polymer, and d_s is the density of the solvent.

RESULTS AND DISCUSSION

Reaction of PGA with Triethylene Glycol Monoethyl Ether (TEGME)

To confirm that the curing process of the heterogeneous network polymers is effected by the esterification of the γ-carboxyl groups of PGA with the hydroxyl groups of PEG, the following model experiments were undertaken. PGA was allowed to react with the monofunctional TEGME in DMF; the reaction conditions were the same as those under which the heterogeneous network polymers were synthesized. Yellow translucent films (abbreviated PGA-TEGME) were obtained after complete evaporation of DMF and unreacted TEGME; evaporation of a substantial portion of TEGME could not be avoided because its boiling point is 248°C.

In Table I are shown the mole ratios of the hydroxyl group in TEGME to the

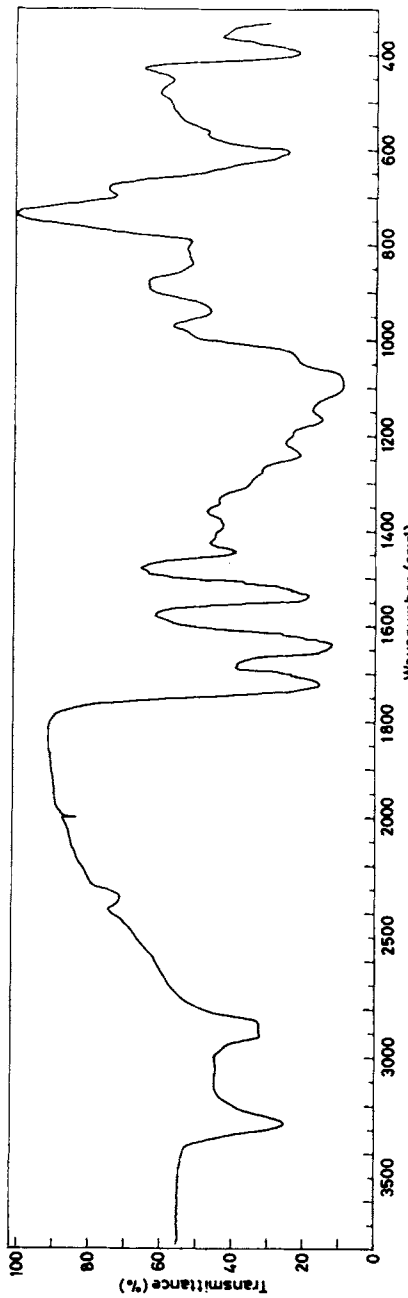

Fig. 1. Infrared spectrum of PGA-TEGME (no. 3) measured by multiple internal reflection method.

carboxyl group in PGA in the original reaction mixtures and the elemental analyses of the films that were extracted with DMF at room temperature for seven days. From the observed carbon contents, the degrees of esterification, ρ, were calculated under the assumption that the incorporation of TEGME into PGA as unextractable was effected exclusively by the esterification of γ-carboxyl groups of PGA. From those ρ values, the elemental analyses for H and N were back-calculated. The agreement between the found and the calculated values appears to verify the above assumption and the effectiveness of the extraction of the unreacted polyethers with DMF at room temperature.

In Table I, the larger $1/K$ became the more TEGME remained in contact with PGA during the course of reaction even if the evaporation of TEGME had to be taken into account. The fact that the larger $1/K$ gave rise to the considerably increased degree of esterification suggests that eventually nearly quantitative esterification might be accomplished with a completely unvolatile polyether glycol.

Figure 1 shows the infrared spectrum of PGA-TEGME (no. 3) measured by a multiple internal reflection (MIR) method. The amide I, II, and V bands appear at 1645, 1540, and 600 cm^{-1}, respectively. These bands are characteristic of polypeptide chains which exist in α-helix conformation. A strong band at around 1090 cm^{-1} arises from the C—O—C stretching vibration of TEGME.

Characterization of Heterogeneous Network Polymers

Table II shows the mole ratio K of the carboxyl groups in PGA to the hydroxyl groups in PEG in the reaction mixtures, the density d, the gel percent g, the

TABLE II
Characterization of Heterogeneous Network Polymers

	K[a]	d,[b] g/cm³	g,[c] %	q[d]	$\nu \times 10^3$,[e] mole/g	$C \times 10^3$,[f] mole/g
PGA-PEG300(40/60)	0.85	1.283–1.303	91.5–92.4	1.70–1.74	3.4	0
PGA-PEG300(50/50)	1.28	1.276–1.296	93.0–96.4	1.62–1.63	2.9	1.1
PGA-PEG300(60/40)	1.90	1.306–1.308	96.7–99.0	1.61–1.88	2.3	2.3
PGA-PEG300(65/35)	2.38	1.310–1.322	98.5–99.7	1.68–1.73	2.1	2.9
PGA-PEG300(70/30)	2.98	1.326–1.339	98.6–99.5	1.88–1.92	1.8	3.6
PGA-PEG600(30/70)	0.95	1.283–1.285	76.3–77.6	2.26–2.33	2.3	0.7
PGA-PEG600(40/60)	1.47	1.278–1.300	78.2–91.8	1.72–2.56	2.0	1.3
PGA-PEG600(50/50)	2.21	1.278–1.305	89.3–96.2	1.84–2.19	1.7	2.3
PGA-PEG600(60/40)	3.31	1.304–1.309	97.4–99.4	1.97–2.05	1.4	3.3
PGA-PEG600(65/35)	4.10	1.314–1.323	97.3–99.8	1.99–2.34	1.2	3.8
PGA-PEG600(70/30)	5.16	1.336–1.346	98.5–99.3	2.27–2.51	1.0	4.4
PGA-PEG900(30/70)	1.46	1.271–1.287	74.5–75.6	2.34	1.4	1.3
PGA-PEG900(40/60)	2.28	1.281–1.300	80.1–94.7	1.89–2.33	1.3	1.8
PGA-PEG900(50/50)	3.41	1.287–1.304	82.3–94.8	2.15–2.79	1.1	2.9
PGA-PEG900(60/40)	5.11	1.308–1.310	96.9–98.8	2.20–2.34	0.88	3.8
PGA-PEG900(65/35)	6.33	1.317–1.325	97.6–99.3	2.25–2.70	0.78	4.3
PGA-PEG900(70/30)	7.96	1.318–1.338	97.4–99.0	2.46–2.80	0.66	4.8
PGA-PEG1800(50/50)	7.09	1.282	91.4–94.8	2.60	0.51	3.4
PGA-PEG1800(70/30)	16.6	1.308	94.8	3.43	0.30	5.2

[a] K = [—COOH]/[—OH], mole ratio of carboxyl groups in PGA to hydroxyl groups in PEG in reaction mixtures.

[b] Density, measured by a floation method using carbon tetrachloride and cyclohexane at 25°C.

[c] Gel per cent, in DMF at 25°C.

[d] Swelling ratio, in DMF at 25°C.

[e] Crosslink density.

[f] Concentration of free carboxyl groups.

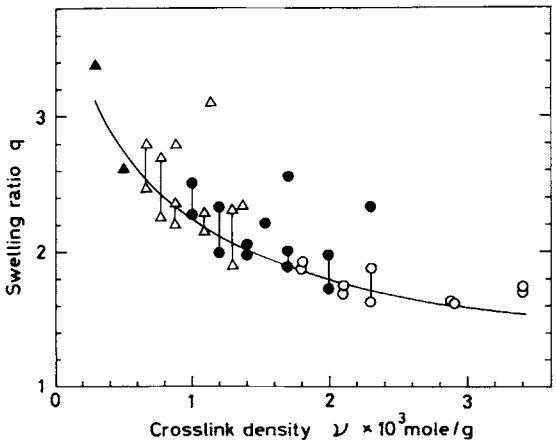

Fig. 2. Plot of swelling ratio vs crosslink density: (○) PGA-PEG300; (●) PGA-PEG600; (△) PGA-PEG900; (▲) PGA-PEG1800.

swelling ratio q, the crosslink density ν, and the concentration of the free carboxyl groups C. For d, g, and q are shown the upper and lower limit values that were obtained from the measurements made on many samples of the same compositions. The ν and C values were determined by the equations below under the assumption that the sol consisted only of PEG:

$$\nu = \frac{2(g-x)}{\mathrm{M}\cdot g}\ \mathrm{mole/g}, \qquad C = \left\{\frac{x}{129} - \frac{2(g-x)}{\mathrm{M}}\right\} \times \frac{1}{100}\ \mathrm{mole/g}$$

where x is the weight percent of PGA and M is the molecular weight of PEG. As Figure 2 illustrates, q decreases gradually as ν increases. A smooth curve may be drawn, within the limits of experimental errors, for the heterogeneous network polymers composed of PEG of different molecular weights. The data points in Figure 2 that deviate extremely upward are those from polymers whose gel per cents were less than 90%; this is indicative of the formation of ineffective networks in such polymers. Exclusing these, we may conclude that the heterogeneous networks were actually formed, for q depends chiefly on ν.

Figures 3 and 4 show the infrared spectra of PGA, PEG900 and PGA-PEG900 (70/30), respectively. PGA-PEG900 (70/30) has characteristic bands of an α-helix at 1640 cm^{-1} (amide I), 1540 cm^{-1} (amide II), 605 cm^{-1} (amide V) and 395 cm^{-1}. There are also weak characteristic bands of β-form at 1630 cm^{-1}, 700 cm^{-1}, and of random coil at 650 cm^{-1}. A strong band at around 1090 cm^{-1} arises from C—O—C stretching vibration of PEG. Figure 4 is very similar to Figure 1.

We conclude that most of PGA chains of heterogeneous network polymers exist in α-helix form and that the network is formed by esterification.

Dynamic Mechanical Properties

Effect of PGA Content

Figures 5, 6, and 7 show the dynamic mechanical properties of heterogeneous network polymers as a function of PGA content. As the PGA content increases

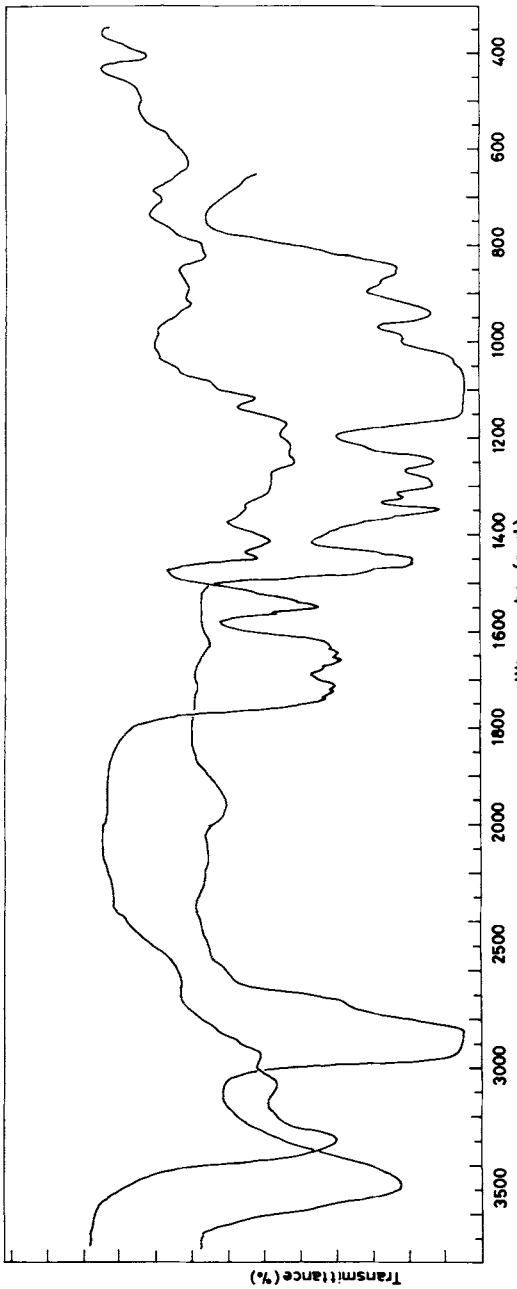

Fig. 3. Infrared spectra of PGA and PEG900.

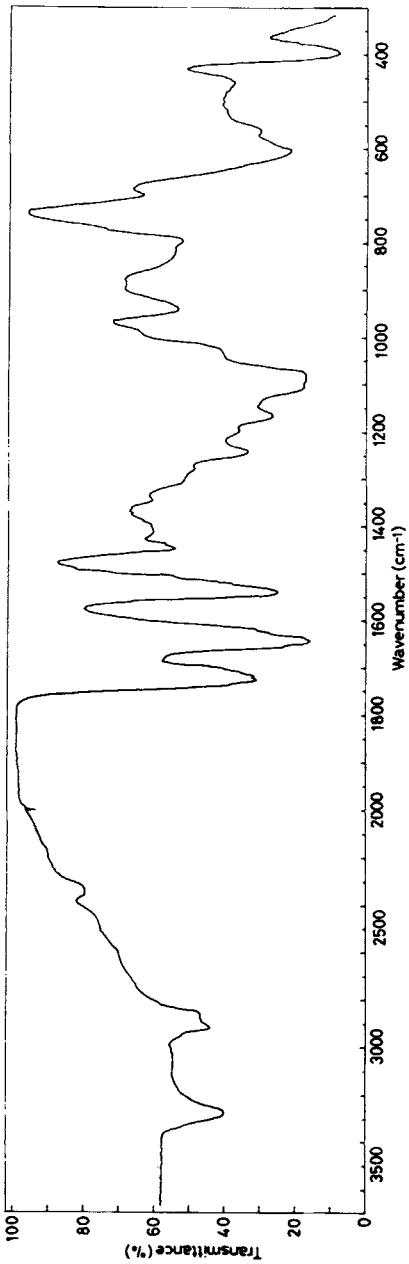

Fig. 4. Infrared spectrum of PGA-PEG900 (70/30) measured by multiple internal reflection method.

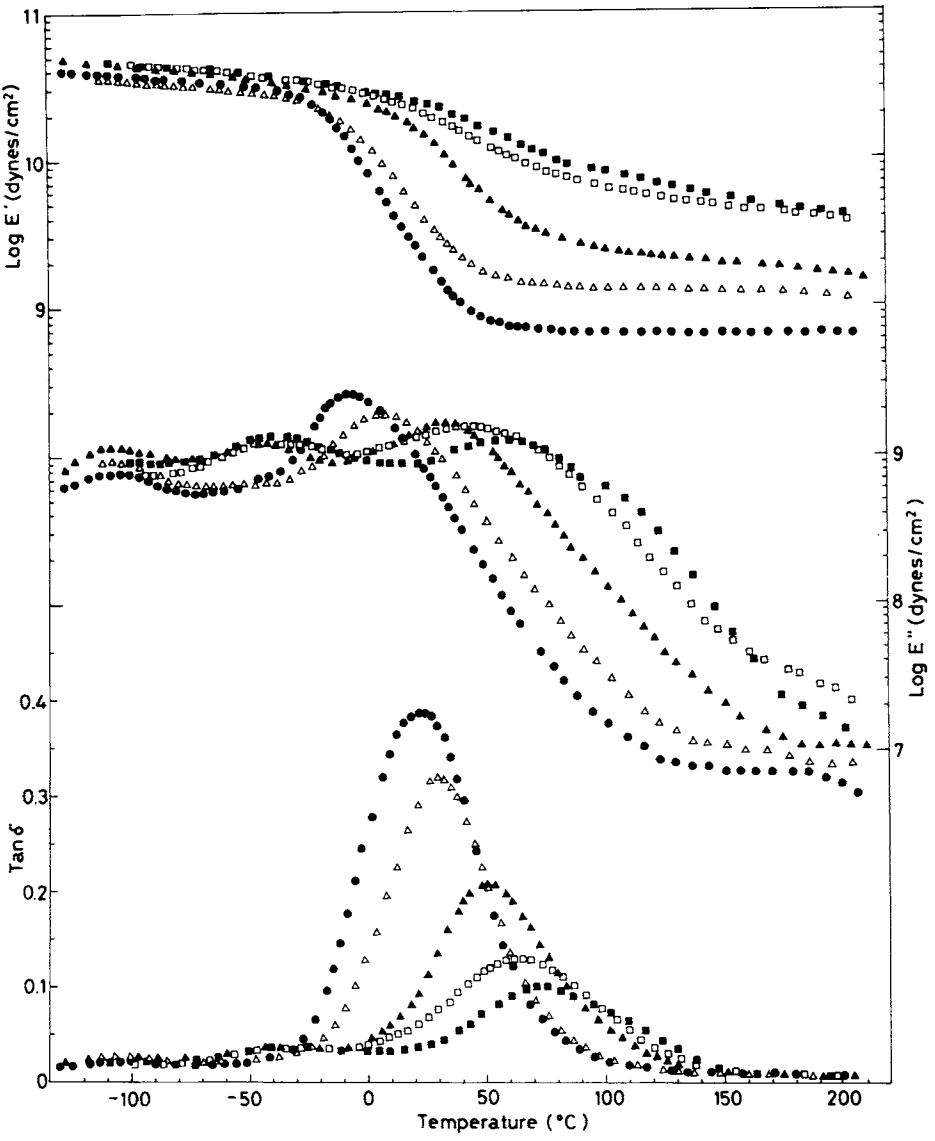

Fig. 5. Dependence of dynamic mechanical properties of PGA-PEG300 on PGA content; (●) PGA-PEG300 (40/60); (△) PGA-PEG300 (50/50); (▲) PGA-PEG300 (60/40); (□) PGA-PEG300 (65/35); (■) PGPEG300 (70/30).

from 30% to 70% while the molecular weight of PEG is kept constant, (1) the peak temperatures of tan δ and E'' shift to higher temperatures; (2) tan δ and E'' curves broaden and decrease in magnitude; (3) E' above the transition region increases. These crosslinked polymers have relatively high moduli; even the lowest E' in the series exhibited by PGA-PEG900 (30/70) had a value of 3×10^8 dynes/cm^2.

Figure 8 is a recapitulation of the above observation (1); a sharp break at around 60% PGA content is obvious. An interpretation of the above dynamic mechanical behavior follows. The increase in the content of PGA (hard com-

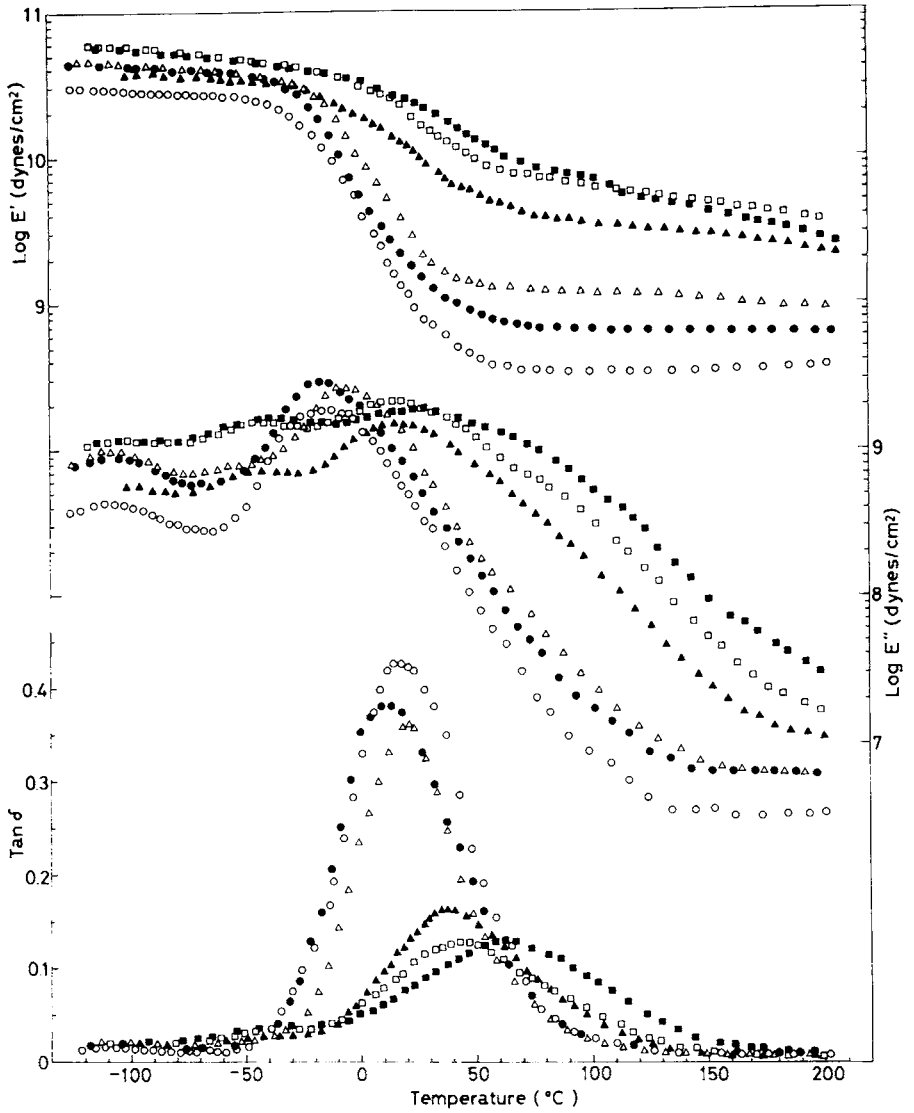

Fig. 6. Dependence of dynamic mechanical properties of PGA-PEG600 on PGA content; (○) PGA-PEG600 (30/70); (●) PGA-PEG600 (40/60); (△) PGA-PEG600 (50/50); (▲) PGA-PEG600 (60/40); (□) PGA-PEG600 (65/35); (■) PGA-PEG600 (70/30).

ponent) naturally raised the peak temperatures of tan δ and E'' owing to a copolymer effect. There remains one point to be mentioned, however. If we increase the PGA content while keeping the molecular weight of PEG constant, as we did in this work, we are simultaneously decreasing the concentration of crosslink points as evidenced in Table II. The decrease in crosslink density would cause a depression of the peak temperatures of tan δ and E''—the reverse of what was observed. In this respect, we previously demonstrated that the copolymer effect predominates over the crosslinking effect in our heterogeneous network polymer system.[8,9]

In general, the dynamic mechanical properties of a composite material depend

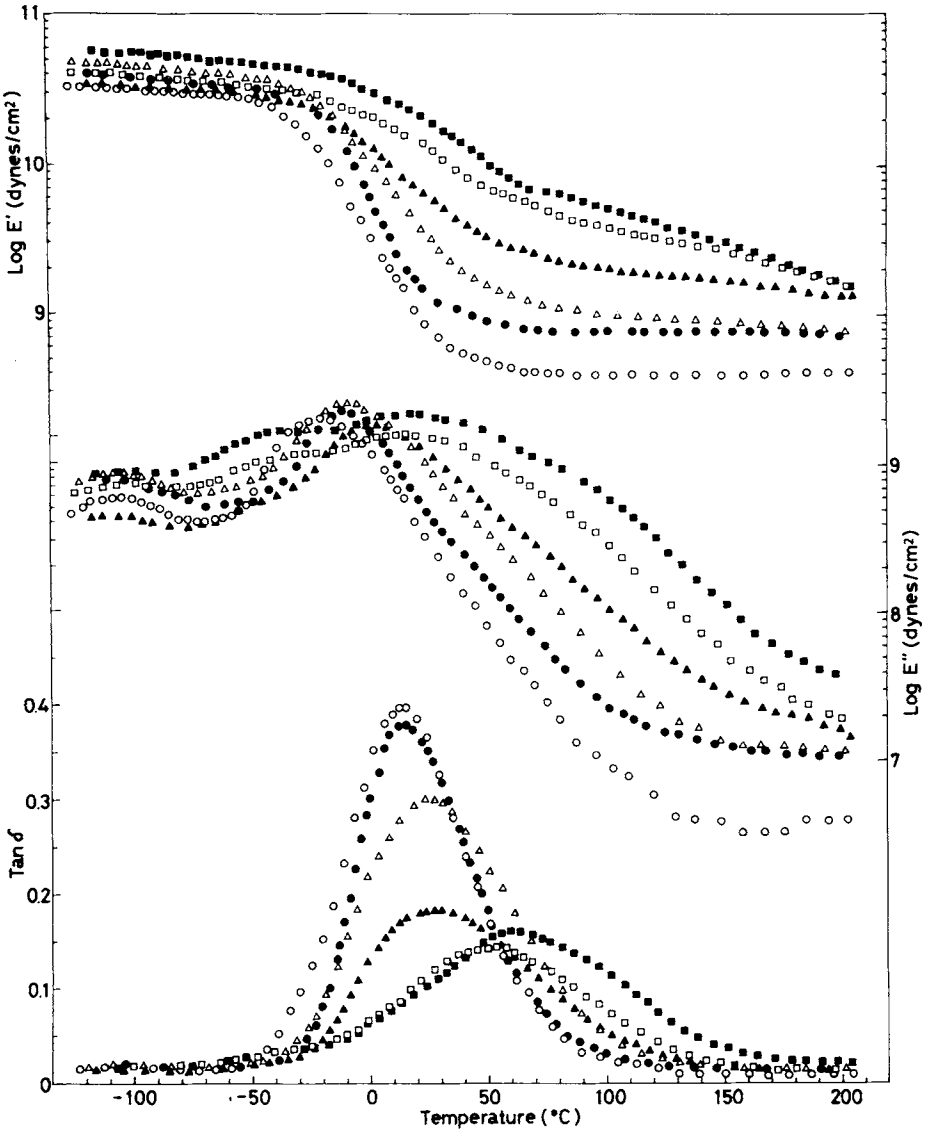

Fig. 7. Dependence of dynamic mechanical properties of PGA-PEG900 on PGA content; (○) PGA-PEG900 (30/70); (●) PGA-PEG900 (40/60); (△) PGA-PEG900 (50/50); (▲) PGA-PEG900 (60/40); (□) PGA-PEG900 (65/35); (■) PGA-PEG900 (70/30).

greatly on the nature of the continuous phase.[10] If a rigid component forms the continuous phase, an applied stress will be transmitted through the rigid continuous phase to a soft dispersed phase. If, on the other hand, the continuous phase is made of a soft omponent, the stress will not be effectively transmitted through the soft continuous phase to a rigid dispersed phase. This generalized picture appears to explain well the behavior of our particular network polymer systems, if we assume that a phase inversion takes place at around 60% PGA content. Moreover, our heterogeneous network polymer systems are very similar to segmented polyurethane block copolymers in the following respects: (1) they

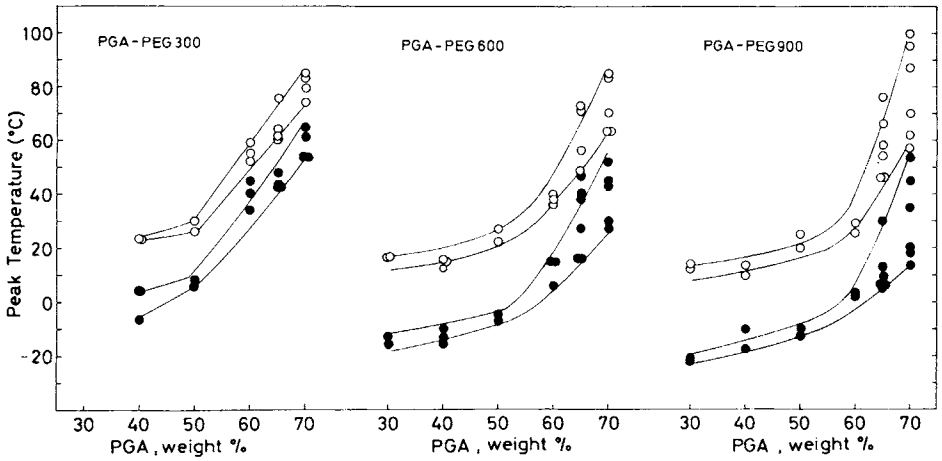

Fig. 8. Plot of peak temperature of tan δ (○) and E'' (●) vs PGA content. Two lines for each of tan δ and E'' indicate upper and lower limits of peak temperature.

consist of a hard and a soft component; (2) the hard component crystallizes and the soft component consists of a polyether; (3) the viscoelastic properties are attributed to the aggregation of the hard component; and (4) the hard-component domains are dispersed in the soft-component matrix, and a phase inversion takes place depending on the composition and the experimental conditions.

Huh et al.[11] studied the dynamic mechanical properties of polyester and polyether polyurethane block copolymers. They found that the glass transition temperatures were greatly influenced by the molecular weight of the soft component, the content of the hard component, and the thermal history. They assigned the relaxation process to the micro-Brownian motions of amorphous macroglycol segments. The effects of these influencing factors are very similar to our heterogeneous network systems when the PEG content is less than 50%, and a similar explanation may be applicable. That is, when the PGA content is less than 50%, the continuous phase is presumably rich in PEG and the stress is almost exclusively carried by this soft continuous phase. Consequently, the relaxation has its origin in the micro-Brownian motions of the PEG segments; the tan δ curves are nearly symmetric around the peak temperatures, and their heights decrease as the PEG content decreases. With the increase in PGA content, the peak temperatures of tan δ and E'' shift to higher temperatures but slightly, because the increase in the content of PGA occurs almost exclusively in the dispersed phase. On the other hand, if the PGA content exceeds 60%, PGA, in turn, becomes the major constituent of the continuous phase. The relaxation arises not only from the micro-Brownian motions of the PGA segments in the disordered regions but also from the PEG segments. As a result, the tan δ curves become broad and unsymmetric. With the increase in the PGA content, the peak temperatures of tan δ and E'' shift to higher temperatures considerably because the increase in the PGA content occurs in the continuous phase.

A small peak is also recognized in E'' curves at $-35° \sim -45°C$; this is probably due to the micro-Brownian motions of the unconstrained PEG segments that are remote from the crosslink points. The high moduli ($E > 3 \times 10^8$ dynes/cm^2) that are observed above the transition region are probably due to the fact that

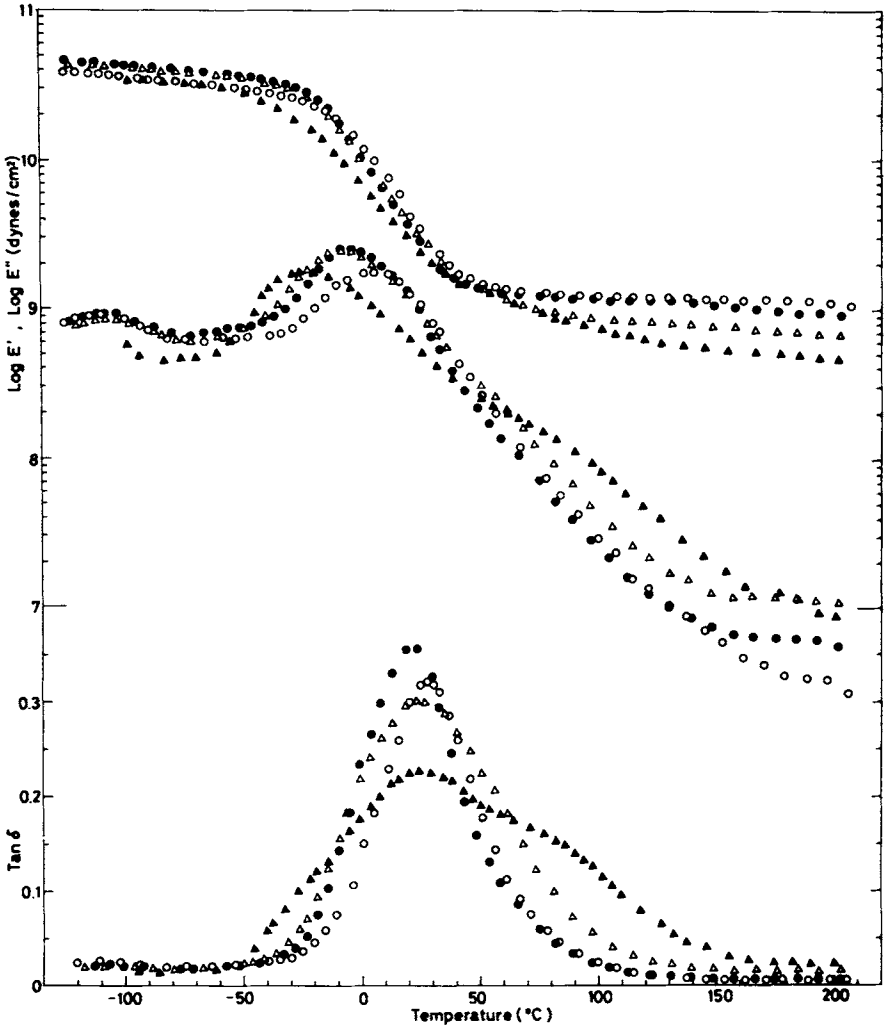

Fig. 9. Dependence of dynamic mechanical properties of PGA-PEG (50/50) on molecular weight of PEG; (○) PGA-PEG300 (50/50); (●) PGA-PEG600 (50/50); (△) PGA-PEG900 (50/50); (▲) PGA-PEG1800 (50/50).

the PGA component retains its rigid, rod-like α-helix conformation up to ca. 200°C.

At this point it may be worth reviewing some of the recent results reported for the viscoelastic behavior of polypeptide films.[12–25] In the studies on poly(γ-methyl D-glutamate) (PMDG), Kajiyama et al.[23,24] observed two kinds of crystalline relaxation processes in the temperature ranges of 150°–170°C (α_1 relaxation) and 180°–190°C (α_2 relaxation). They attributed the α_1 relaxation to shear deformation in the interhelix region of the crystals and the α_2 relaxation to tensile or bending deformations of the α-helix. They also assigned the β relaxation occurring at 100°–120°C to the micro-Brownian motions in the disordered region. Our previous study on a PGA film cast from N,N-dimethylformamide at 100°C showed the existence of a tan δ peak at ca. 135°C.[8] This

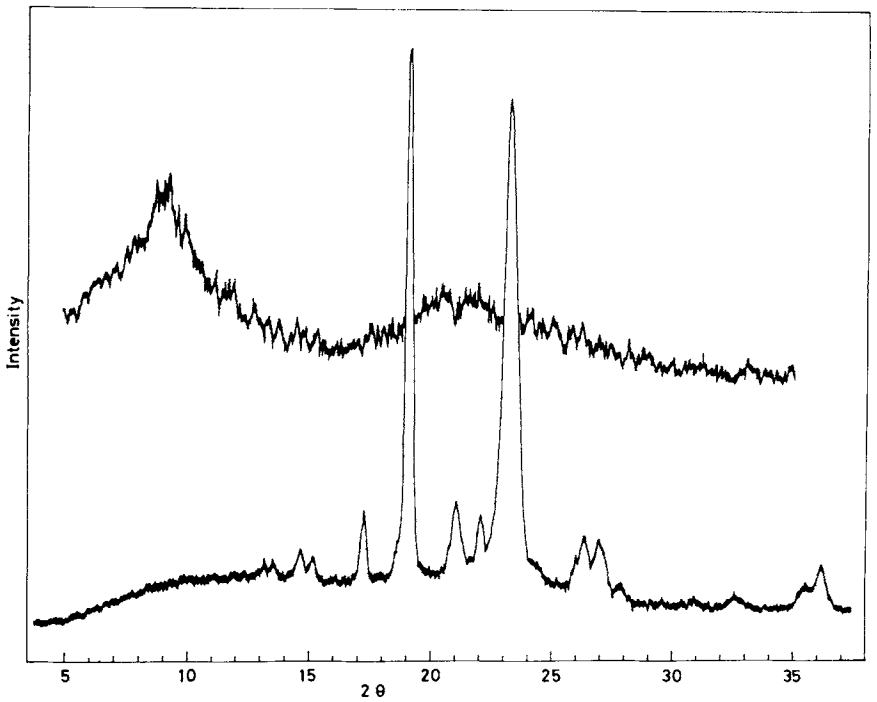

Fig. 10. Wide-angle x-ray diffraction patterns of PGA and PEG1800.

relaxation is now believed to correspond to the β relaxation of PMDG reported by Kajiyama et al.

Nguyen et al.[21] also reported the dynamic mechanical properties of PGA; however, their tan δ curve appeared quite different from ours. The discrepancy seems to have arisen from the water contained in the PGA film; for we, too, obtained a tan δ curve very similar to theirs when the film was deliberately allowed to absorb some moisture. In any event, PGA has a relaxation at around 135°C. Furthermore, as will be mentioned later, polarizing microscopic observations of heterogeneous network polymers at higher temperatures showed that bright regions existed up to 190° ± 10°C. This suggests that the ordered regions were not relaxed up to this temperature. Thus, we are inclined to believe that the observed relaxation of the heterogeneous network polymers with the PGA content larger than 60% is a superposition of the relaxations due to micro-Brownian motions of PEG segments (soft component) and those of PGA segments in the disordered regions.

Effects of Crosslink Density and Free Carboxyl Group Content

So far, we have been discussing the effect of PGA content while the molecular weight of PEG was kept constant. In this section, the situation is reversed; namely, we will discuss the effect of varying PEG molecular weight while the PGA content remains constant. An increase in the PEG molecular weight gives rise simultaneously to a decrease in crosslink density and an increase in the content of free carboxyl groups, as can be seen in Table II. According to Figures 8 and 9, an increase in the PEG molecular weight causes the following: (1) the peak

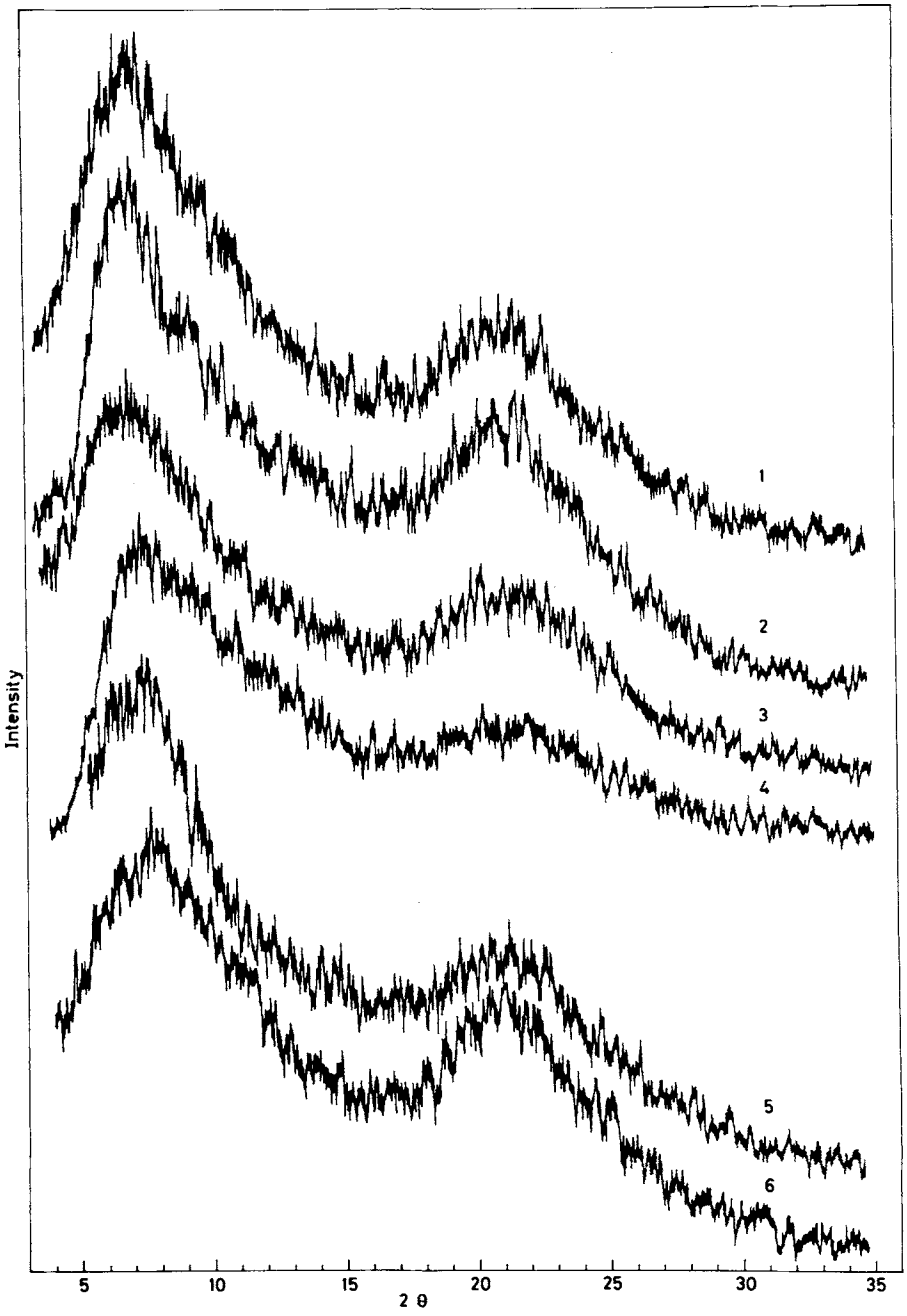

Fig. 11. Wide-angle x-ray diffraction patterns of (1) PGA-PEG600 (30/70), (2) PGA-PEG600 (40/60), (3) PGA-PEG600 (50/50), (4) PGA-PEG600 (60/40), (5) PGA-PEG600 (65/35), (6) PGA-PEG600 (70/30).

temperatures of tan δ and E'' shift to slightly lower temperatures; (2) the magnitude of E' above the transition regions decreases but slightly.

Ordinarily, crosslinking and hydrogen bonding influence very much the dynamic mechanical properties of a polymer above its transition temperature. In

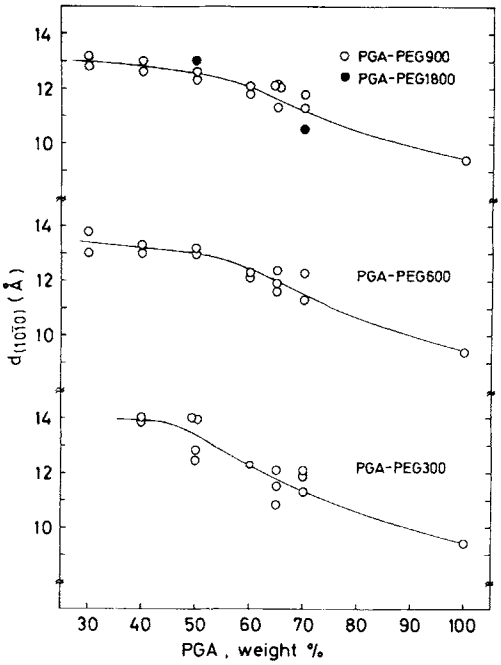

Fig. 12. Plot of $d_{10\bar{1}0}$ vs PGA content.

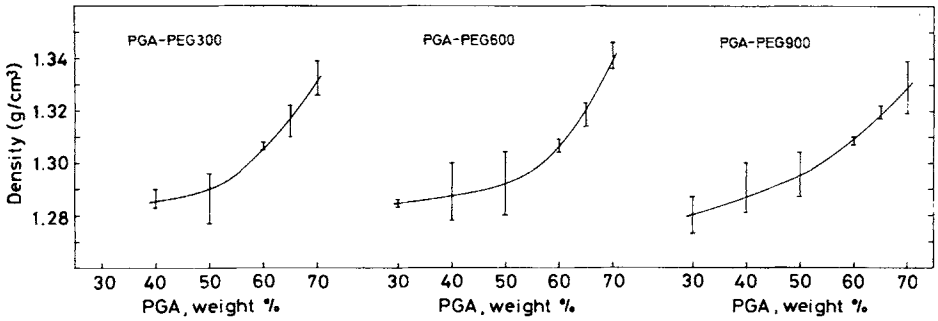

Fig. 13. Plot of density vs PGA content.

our heterogeneous network polymers, however, a decrease in crosslink density is always accompanied by an increase in hydrogen bonding due to the free carboxyl groups. Consequently, these two factors must cancel each other out to some extent. Observations (1) and (2) indicate that the effect of crosslink density is somewhat greater than that of the hydrogen bonding. In Figure 9, the existence of two tan δ peaks is recognized for PGA-PEG1800 (50/50). This suggests that when the PEG chain becomes very long, an extensive phase separation occurs.

X-Ray Diffraction

The state of aggregation affects very much the dynamic mechanical behavior of a composite system. In our PGA–PEG systems, the state of aggregation is

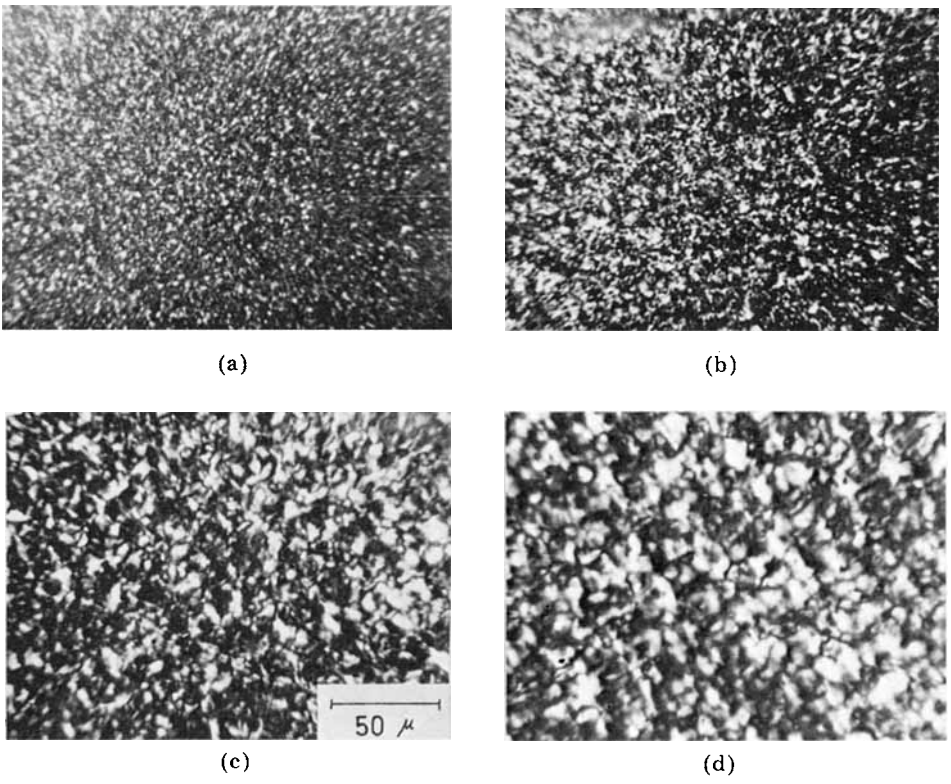

Fig. 14. Polarizing micrographs of PGA-PEG300: (a) PGA-PEG300 (40/60); (b) PGA-PEG300 (50/50); (c) PGA-PEG300 (60/40); (d) PGA-PEG300 (70/30).

governed by our choice of the composition, the relative amount of solvent used for sample preparation, and the rate of solvent evaporation, etc. To study the state of aggregation or the domain structures, we made use of wide-angle x-ray diffractions and polarizing microscopy. Figures 10 and 11 show x-ray diffraction patterns of PGA, PEG1800, and heterogeneous network polymers, respectively. PGA has a reflection at a Bragg angle of 2θ = ca. 9.3°, which is characteristic of the α-helix crystal structure.[26] PEG1800 has strong reflections at Bragg angles of 2Θ = 17.0° (*s*), 18.8° (*vs*), 20.8° (*s*), and 23.1° (*vs*). We previously claimed, on the basis of wide-angle x-ray diffraction photographs, that PGA-PEG300 (60/40), 600 (60/40), 900 (60/40), and 1800 (60/40) were noncrystalline.[9] But the scintillation counting x-ray diffraction patterns given in Figure 11 indicate that every heterogeneous network polymer has a reflection at a Bragg angle of 2θ = 6°–9°, which probably corresponds to the $(10\bar{1}0)$ plane of the α-helix crystal form of PGA. Since the α-form crystal structure of PGA has not yet been determined, one might argue that the Bragg spacing could not necessarily be assigned to $(10\bar{1}0)$ spacing. Nevertheless, the α-helix crystal structure of poly(γ-methyl glutamate) is known.[27]

When PMDG is subject to partial hydrolysis, a linear relationship holds between the degree of hydrolysis and the α-helix spacing based on x-ray measurements.[28] By analogy, our assignment of the Bragg angle 2θ = 6°–9° to the $(10\bar{1}0)$ spacing seems reasonable. The lattice distance, $d_{10\bar{1}0}$, is plotted against the PGA content in Figure 12. A distinct break is recognized here again between

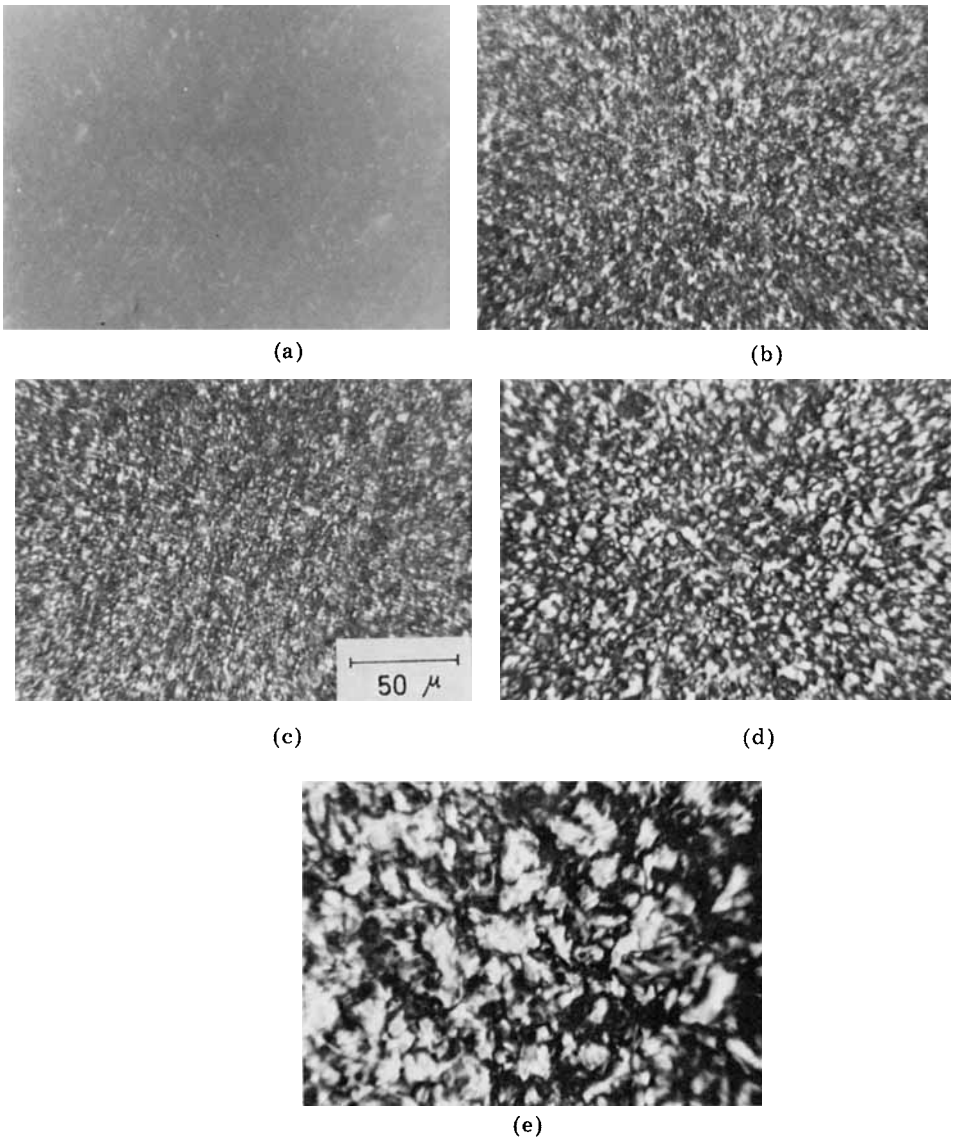

Fig. 15. Polarizing micrographs of PGA-PEG600: (a) PGA-PEG600 (30/70); (b) PGA-PEG600 (40/60); (c) PGA-PEG600 (50/50); (d) PGA-PEG600 (60/40); (e) PGA-PEG600 (70/30).

50% and 60% PGA. Since $(2/\sqrt{3}) \times d_{10\bar{1}0}$ corresponds to the distance between neighboring α-helices, the above observation means that the interhelix distance spreads gradually apart up until 40% PEG and suddenly becomes almost constant after a PEG content of ca. 50% is reached.

The density of heterogeneous network polymer is plotted against the PGA content in Figure 13. Also in this case, a break point is recognized between 50% and 60%.

It is well known that synthetic polypeptides form a cholesteric liquid crystal in various solvents,[29,30] and the cholesteric structure is retained also in the solid films prepared by evaporation of the solvents.[30–33] Friedman et al.[31] showed

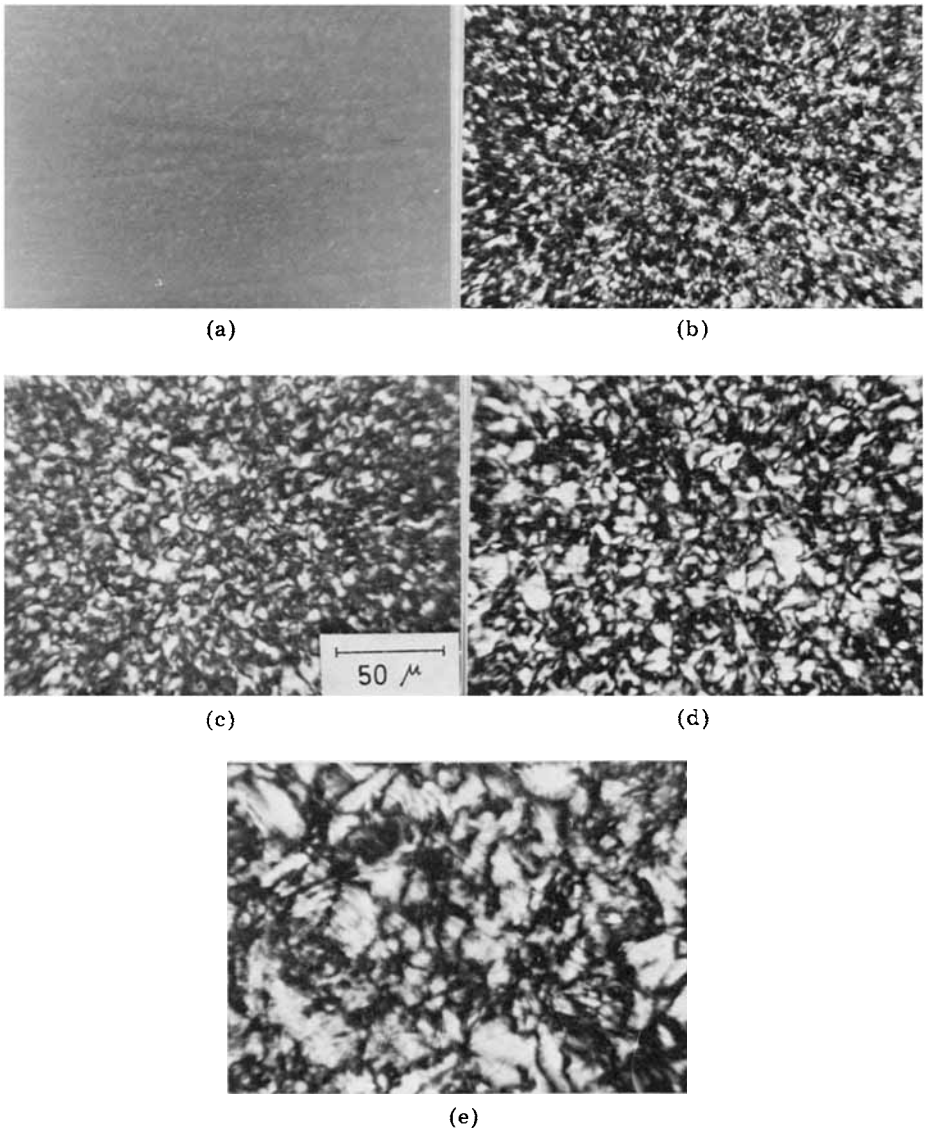

Fig. 16. Polarizing micrographs of PGA-PEG900: (a) PGA-PEG900 (30/70); (b) PGA-PEG900 (40/60); (c) PGA-PEG900 (50/50); (d) PGA-PEG900 (60/40); (e) PGA-PEG900 (70/30).

that solid PGA which was plasticized with 35% 3,3′-dimethylbiphenyl possessed a domain texture of parallel-packed chains. Moreover, Samulski et al.[33] showed that the cholesteric structure does exist in solid poly(γ-benzyl L-glutamate) (PBDG) plasticized with chlorinated polyphenyls; $d_{10\bar{1}0}$ spacing expands with an increase in the plasticizer content, but when the volume fraction of the plasticizer exceeds 0.5, $d_{1\bar{1}0}$ spacing stops expanding. In view of these properties of PGA and other polypeptides, we propose the following mechanism of microphase separation and the phase inversion in our heterogeneous network polymers which is consistent with the observed dynamic mechanical behavior, x-ray diffractions, and the densities.

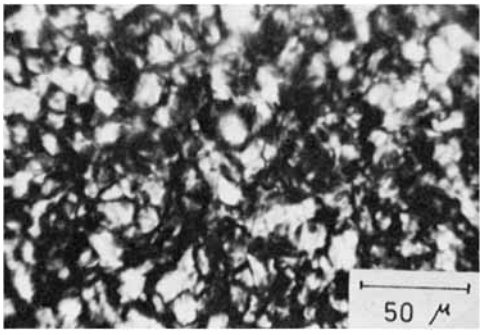

(a)

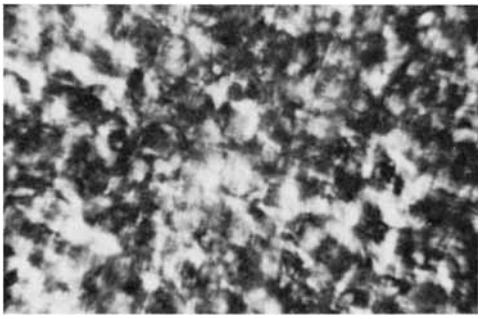

(b)

Fig. 17. Polarizing micrographs of PGA-PEG1800: (a) PGA-PEG1800 (50/50); (b) PGA-PEG1800 (70/30).

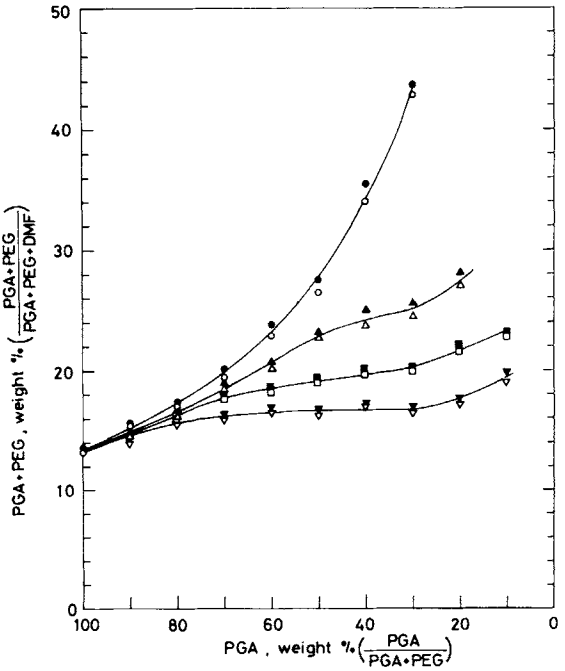

Fig. 18. Plot of composition of A point at 30°C vs PGA content. The concentration is expressed by PGA + PEG concentration. Filled and open marks indicate anisotropic and isotropic regions, respectively: (○) PGA-PEG300-DMF; (△) PGA-PEG900-DMF; (□) PGA-PEG1800-DMF; (▽) PGA-PEG4000-DMF.

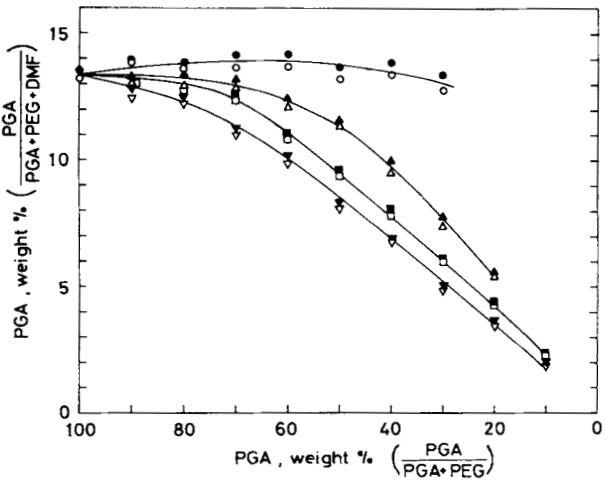

Fig. 19. Plot of composition of A point at 30°C vs PGA content. The concentration is expressed by PGA concentration. Filled and open marks indicate anisotropic and isotropic regions, respectively: (○) PGA-PEG300-DMF; (△) PGA-PEG900-DMF; (□) PGA-PEG1800-DMF; (▽) PGA-PEG4000-DMF.

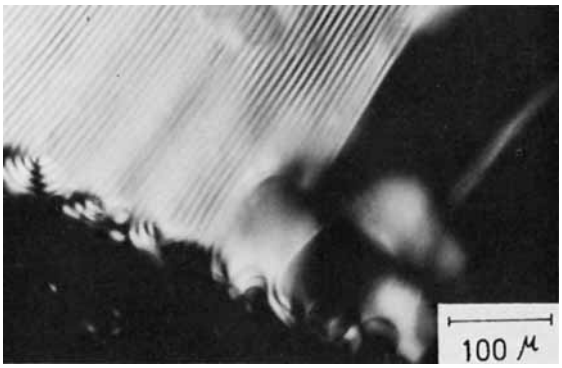

Fig. 20. Polarizing micrographs of PGA-PEG900-DMF [PGA/PEG = 70/30, (PGA + PEG)/(PGA + PEG + DMF) × 100 = 18.5%].

Fig. 21. Polarizing micrographs of PGA-PEG900 (70/30).

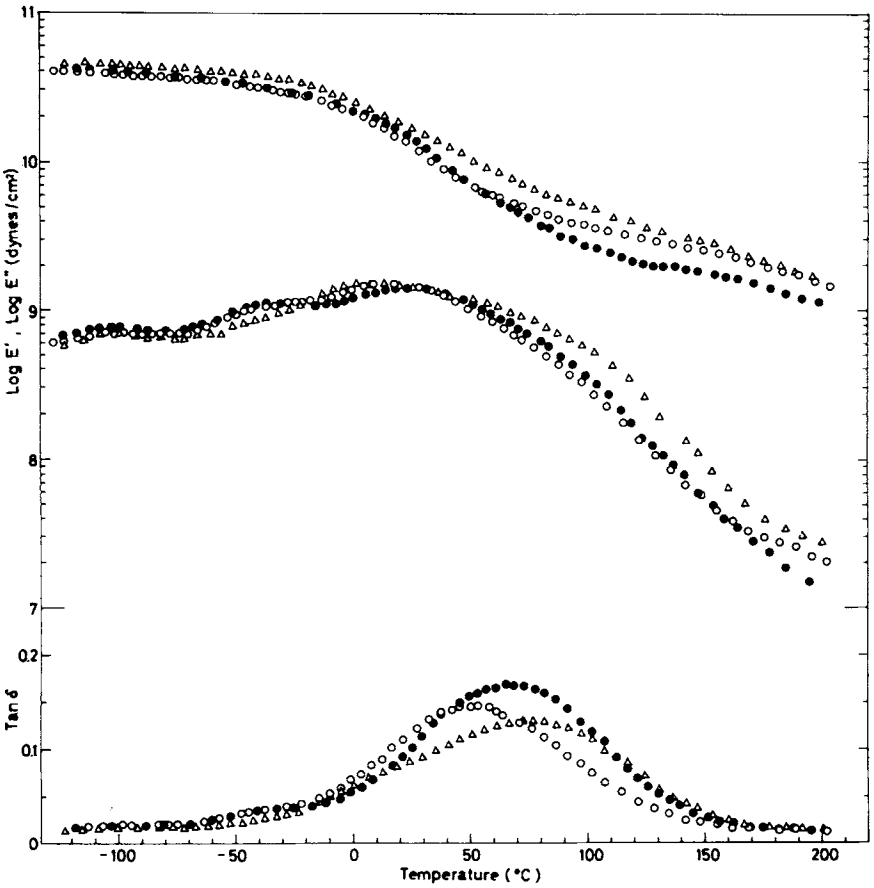

Fig. 22. Dynamic Mechanical Properties of PGA-PEG900 (65/35): (○) PGA-PEG900 (65/35); (●) PGA-PEG900 (65/35); (△) PGA-PEG900 (65/35).

The DMF solution of PGA and PEG is concentrated as the DMF evaporates, and the PGA α helix chains aggregate or form liquid crystals. The PEG chains, which are now chemically bound to PGA, are sandwiched by the PGA helices or curl around the PGA helices owing to hydrogen bonding between the carboxyl groups of PGA and the ether linkages of PEG. So far, as the PGA content is larger than 60%, most PEG chains can be accommodated within the interhelical regions of PGA. If the PGA becomes as lean as 50% or less, a considerable proportion of PEG cannot associate with PGA and forms a continuous phase; as a result, $d_{10\bar{1}0}$ no longer increases.

Polarizing Microscopy

The photographs of the heterogeneous network polymers taken under a polarizing microscope are shown in Figures 14–17. Optically anisotropic regions are present in every specimen except PGA-PEG600 (30/70) and 900 (30/70). The anisotropic regions exist up to 190° ± 10°C. The dimension and the concentration of the anisotropic regions decrease as the content of PGA decreases. When the PGA content is 70%, the size of bright spots is ca. 10–30 microns. If

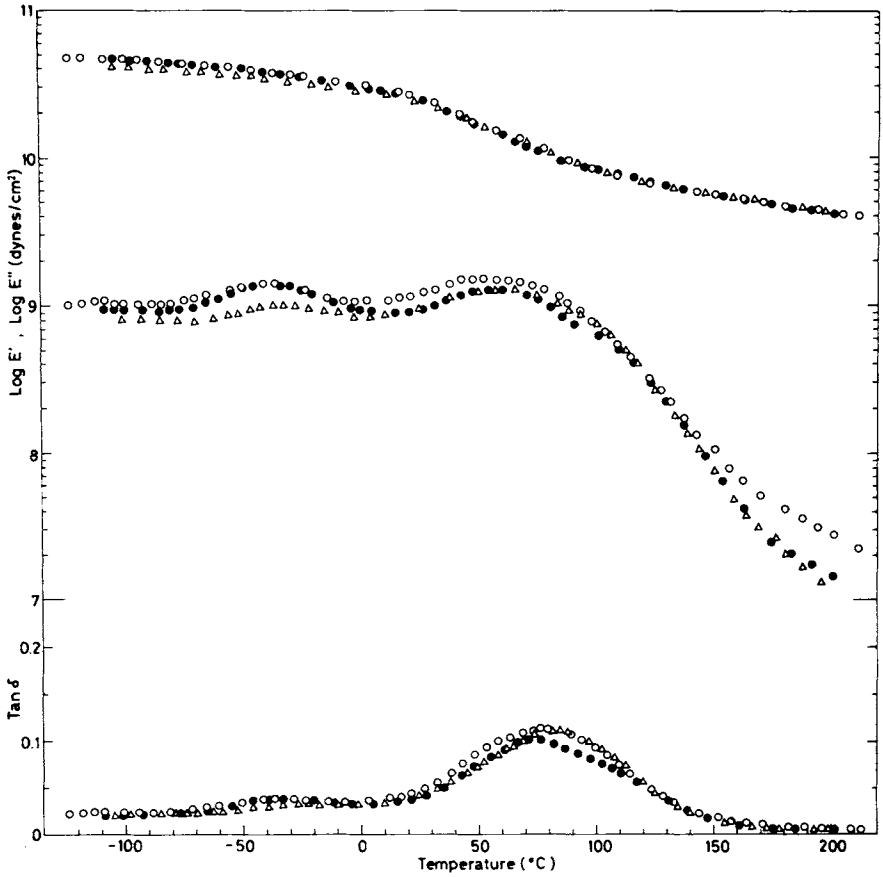

Fig. 23. Dynamic mechanical properties of PGA-PEG300 (70/30): (○) PGA-PEG300 (70/30); (●) PGA-PEG300 (70/30); (△) PGA-PEG300 (70/30).

the specimens are rotated, the bright and dark regions invert. This suggests that most of the domains are oriented and that the direction of orientation of each region varies. On the other hand, when the PGA content is 40%, the size of bright spots becomes smaller than a few microns and isotropic regions do exist; for some regions that remain dark no matter how the specimens are rotated are observed.

The heterogeneous network polymer films consisting of 30% PGA and 70% PEG are transparent and almost dark under a polarizing microscope. The results of the polarizing microscopic observations provide more supporting evidence for the inversion of phase separation in these systems. At 70% PGA content, the rod-like α-helix chains of PGA aggregate, occluding most of the PEG chains around them to form the optically anisotropic regions. At 40% PGA, part of the PEG chains cannot be incorporated and they separately form the isotropic regions. At 30% PGA, the anisotropic regions due to PGA are so finely dispersed that the film becomes optically isotropic and transparent.

In order to elucidate the mechanism of phase separation and phase structure, it may be necessary to investigate the liquid crystals of the PGA–PEG–DMF system. We found that the PGA–PEG–DMF system also formed a liquid crystal.

In Figures 18 and 19, the composition of the solution corresponding to the A point, at which an anisotropic phase separates from an isotropic solution, was plotted against the composition of a PGA–PEG mixture that was dissolved in DMF. Figure 20 shows polarizing micrographs of PGA-PEG900-DMF [PGA/PEG = 70/30, (PGA + PEG)/(PGA + PEG + DMF) × 100 = 18.5%] in a thin (0.15–0.18 mm) rectangular cell. The appearance of alternating bright and dark lines suggests that a cholesteric structure does exist.

The polarizing micrographs of heterogeneous network polymers are shown in Figures 14–17, but photographs having alternating bright and dark lines were sometimes obtained (Fig. 21). This indicates that a cholesteric structure persists in heterogeneous network polymers. The difference of the evaporation rate of the solvent may be a cause for the difference between Figures 14–17 and 21. Detailed studies of the liquid crystals of the PGA–PEG–DMF system are now in progress.

Reproducibility of Data

The reproducibility of dynamic mechanical, x-ray diffraction, and polarizing microscopic data was generally good for the heterogeneous network polymers containing less than 50% PGA. But, it was not so good when the PGA content was 65% or 70%. For example, three quite different sets of relaxation curves were obtained with three samples from different runs of preparation with the same composition, as shown in Figure 22. At a fixed PGA content, the reproducibility was better with the polymers containing PEG300 than with those containing PEG900, as can be seen in Figure 23. These trends may be ascribed to the difference in superstructure caused by the variation of the evaporation rate of DMF. Namely, the optically anisotropic regions are finely dispersed at a PGA content below 50%, whereas they are large and irregular when the PGA content was 65% or 70%, as shown in Figures 14–17. The superstructure in the latter case must be much more sensitive to minor fluctuations in the conditions of film preparations, e.g., rate of solvent evaporation, than in the former.

Despite the considerable scatter of the plots in Figures 8 and 12 due to the superstructure variations discussed above, there still is no doubt that there is a sudden change between 50% and 60% PGA content. Studies concerning the effect of the evaporation rate of DMF on the dynamic mechanical properties, x-ray diffraction patterns, and polarizing micrographs are in progress.

The authors express their thanks to Dr. R. Tanaka for his very helpful suggestions during the course of this study. PMDG used in this study was kindly supplied by Ajinomoto Co., Ltd. This study was supported in part by the Scientific Research Fund of the Ministry of Education of Japan.

References

1. L. Bohn, *Rubber Chem. Technol.*, **41**, 495 (1968).
2. B. Schneier, *J. Appl. Polym. Sci.*, **18**, 1999 (1974).
3. E. Hirata, T. Ijitsu, T. Soen, T. Hashimoto, and H. Kawai, *Polymer*, **16**, 249 (1975).
4. Y. J. Chang and G. L. Wilkes, *J. Polym. Sci., Polym. Phys. Ed.*, **13**, 455 (1975).
5. E. Pedemonte, G. Dondero, G. C. Alfonso, and F. Candia, *Polymer*, **16**, 531 (1975).
6. R. W. Seymour, J. R. Overton, and L. S. Corley, *Macromolecules*, **8**, 331 (1975).
7. T. Tanaka, T. Yokoyama, Y. Yamaguchi, M. Furukawa, and T. Mori, *J. Polym. Sci.*, **A-1, 9**, 2745 (1971).

8. T. Mori, Y. Kuchihara, R. Tanaka, and T. Tanaka, *J. Polym. Sci., Polym. Phys. Ed.*, **12,** 501 (1974).
9. T. Mori, R. Tanaka, and T. Tanaka, *J. Polym. Sci., Polym. Phys. Ed.*, **13,** 1633 (1975).
10. T. Miyamoto, K. Kodama, and K. Shibayama, *J. Polym. Sci. A-2,* **8,** 2095 (1970).
11. D. S. Huh and S. L. Cooper, *Polym. Eng. Sci.*, **11,** 369 (1971).
12. R. G. Saba, J. A. Sauer, and A. E. Woodward, *J. Polym. Sci. A-1,* **1,** 1483 (1963).
13. K. Hikichi, K. Saito, M. Kaneko, and J. Furuichi, *J. Phys. Soc. Jpn.*, **19,** 577 (1964).
14. J. V. Koleske and R. D. Lundberg, *Macromolecules,* **2,** 438 (1969).
15. M. Date, T. Takashita, and E. Fukada, *J. Polym. Sci. A-2,* **8,** 61 (1970).
16. A. Hiltner, J. M. Anderson, and E. Borkowski, *Macromolecules,* **5,** 446 (1972).
17. A. Tsutsumi, K. Hikichi, T. Takahashi, Y. Yamashita, N. Matsushima, M. Kanake, and M. Kaneko, *J. Macromol. Sci.-Phys.*, **B8,** 413 (1973).
18. M. Kuroishi, T. Kajiyama, and M. Takayanagi, *Chem. Lett.*, 659 (1973).
19. M. Ichikawa, R. Sakamoto, Y. Abe, and K. Makishima, *Kobunshi Kagaku,* **30,** 346 (1973).
20. T. Noda, Y. Abe, and R. Sakamoto, *Kobunshi Ronbunshu,* **31,** 203 (1974).
21. A. L. Nguyen, B. T. Vu, and G. L. Wilkes, *J. Macromol. Sci.-Phys.*, **B9,** 367 (1974).
22. T. Fukuzawa and I. Uematsu, *Polym. J.*, **6,** 431 (1974).
23. T. Kajiyama, M. Kuroishi, and M. Takayanagi, *J. Macromol. Sci.-Phys.*, **B11,** 121 (1975).
24. T. Kajiyama, M. Kuroishi, and M. Takayanagi, *J. Macromol. Sci.-Phys.*, **B11,** 195 (1975).
25. Y. Yamashita, A. Tsutsumi, K. Hikichi, and M. Kaneko, *Polym. J.*, **8,** 114 (1976).
26. K. Kondo, K. Shimizu, T. Hayakawa, and Y. Go, *Kobunshi Kagaku,* **28,** 510 (1971).
27. C. H. Bamford, A. Elliott, and W. E. Hanby, *Synthetic Polypeptides,* Academic Press, New York, 1956, p. 239.
28. T. Mori, T. Yamada, R. Tanaka, and T. Tanaka, to appear.
29. P. Salujian and V. Luzzati, *Poly-α-Amino Acids,* G. D. Fasman, Ed., Marcel Dekker, New York, 1967, p. 157.
30. E. T. Samulski and A. V. Tobolsky, in *Liquid Crystals and Plastic Crystals,* Vol. 1, G. W. Gray and P. A. Winsor, Eds., Ellis Horwood, Chichester, England, 1974, p. 175.
31. E. Friedman, C. Anderson, R. Roe, and A. V. Tobolsky, *J. Polym. Sci. B,* **10,** 839 (1972).
32. E. T. Samulski and A. V. Tobolsky, *Nature,* **216,** 997 (1967).
33. E. T. Samulski and A. V. Tobolsky, *Mol. Cryst. Liq. Cryst.*, **7,** 433 (1969).

Received August 24, 1976
Revised October 26, 1976